Research Square

Preprints are preliminary reports that have not undergone peer review.
They should not be considered conclusive, used to inform clinical practice,
or referenced by the media as validated information.

Prenatal Cerium Exposure and the Risk of Small-for-Gestational-Age (SGA): Evidence and Early Biomarkers

Jinlei Du
School of Public Health,Baotou Medical College
Lailai Yan
Peking University
Zitong Wang
School of Public Health,Baotou Medical College
Shuai Li
School of Public Health,Baotou Medical College
Yu Qiao
School of Public Health,Baotou Medical College
Lan Luo
School of Public Health,Baotou Medical College
Qi Zhang
School of Public Health,Baotou Medical College
Jianhua Cao
School of Public Health,Baotou Medical College
Dapeng Tai
School of Public Health,Baotou Medical College
Rui Qiao
1257485090qq.com

School of Public Health,Baotou Medical College

Research Article

Keywords: Small for gestational age infants, Ce exposure, miRNA, Early markers, Exosomes

Posted Date: April 23rd, 2026

DOI: https://doi.org/10.21203/rs.3.rs-9186995/v1

License: This work is licensed under a Creative Commons Attribution 4.0 International License.
Read Full License

Additional Declarations: No competing interests reported.

Abstract

Background

During pregnancy, the physiological functions of female individuals undergo changes, and their sensitivity to environmental factors is significantly increased. As the most abundant rare earth element, the biological effects of cerium on pregnancy and early placental development remain unclear. Therefore, prenatal exposure to the rare earth element cerium warrants close attention regarding its effects on pregnancy.

Methods

Pregnant mice were exposed to different doses of cerium nitrate (0, 50, 100, and 200 mg/kg). On gestational day 17 (placental maturation stage), intrauterine pregnancy conditions and placental structural changes were observed. Histopathological alterations in placental tissues were evaluated using hematoxylin and eosin (H&E) staining. Exosomal miRNAs from placental tissues were subjected to miRNA sequencing to identify differentially expressed miRNAs. Gene Ontology (GO) and KEGG enrichment analyses were performed on the dataset. In both in vivo and in vitro models, the expression levels of key components of the MAPK signaling pathway (ARRB2 and p-MAPK14) were determined using qRT-PCR and Western blotting. In human choriocarcinoma cells (JEG-3), cell proliferation under different concentrations of cerium nitrate was assessed using the CCK-8 assay, apoptosis was analyzed by flow cytometry, and IL-6 secretion levels were measured by ELISA.

Results

Prenatal cerium(Ce) exposure increased the proportion of offspring with SGA-like phenotypes. The study found that cerium accumulated in placental tissues, and was accompanied by placental structural alterations and inflammatory cell infiltration. Quantitative PCR further confirmed the coordinated upregulation of miR-483-3p, its host gene IGF2, and the precursor pri-miR-483 in placental tissues. In vitro experiments showed that Ce treatment inhibited the viability of JEG-3 trophoblast cells and promoted IL-6 expression. Moreover, Ce exposure significantly increased the levels of miR-483-3p secreted via exosomes, upregulated the expression of exosome biogenesis-related proteins, and was accompanied by activation of the MAPK/P38 pathway and increased apoptosis.

Conclusion

Maternal cerium exposure was associated with placental injury, inflammatory responses, and SGA-like outcomes in rats. These changes were accompanied by activation of p38 MAPK signaling and upregulation of the IGF2/miR-483-3p locus, as well as increased exosomal miR-483-3p release from

trophoblast cells. Our findings suggest that exosomal miR-483-3p may have potential as an early indicator of Ce-related placental dysfunction, although further validation is required.

1. Introduction

Cerium (Ce) is the most abundant rare earth element and is widely distributed in the environment [1]. With the expanding applications of cerium in industrial and agricultural sectors, environmental concentrations of cerium have steadily increased, thereby elevating the risk of human exposure. An increasing number of studies have reported the potential adverse effects of cerium compounds on human and animal health [2–3]. Current evidence suggests that cerium compounds exhibit multiple toxicological effects, including reproductive toxicity [4], hepatotoxicity [5], and neurotoxicity [6]. However, the immunotoxic effects of cerium remain controversial, and relatively little attention has been paid to other cerium compounds.

Previous studies have shown that crops can accumulate rare earth elements from soil, particularly grasses and leafy plants [7]. Consequently, residents living in rare earth mining areas exhibit significantly elevated levels of rare earth elements in blood, urine, and hair, with blood concentrations reported to be more than 150 times higher than those observed in control populations [8]. Humans can be exposed to rare earth elements, including cerium, through multiple environmental pathways, with dietary intake representing an important exposure route.

Pregnancy is a critical period characterized by heightened susceptibility to environmental exposures. The accumulation of cerium in the maternal body and its potential effects on the placenta–fetus unit may therefore be associated with adverse birth outcomes [9]. Epidemiological studies have suggested that prenatal exposure to light rare earth elements is associated with an increased risk of small-for-gestational-age (SGA) infants, providing population-level evidence that rare earth elements may contribute to abnormal fetal growth [10]. SGA is defined by being under the 10th percentile on a standard growth chart for an infant with the same gestational age and sex as a reference population; Severe SGA is considered anything lower than the third percentile. [11]. It is the main element causing perinatal illness or death and is connected with an increased possibility of experiencing undesirable outcomes, like hampered neurocognitive development and metabolic ailments. [12–13]. In addition to traditional risk factors such as maternal malnutrition, hypertensive disorders of pregnancy, and smoking, environmental exposures have increasingly been recognized as important determinants of impaired fetal growth [14].

The placenta is a critical organ responsible for maternal–fetal substance exchange and the regulation of fetal growth. Structural and functional abnormalities of the placenta are considered key pathological bases of fetal growth restriction and SGA [15].Previous studies suggest that maternal cerium exposure may accumulate in the placenta and impair placental structure and function. These findings raise the possibility that cerium exposure may inhibit embryonic growth[16].The migration and invasion abilities of placental trophoblast cells are essential for spiral artery remodeling and the establishment of adequate

placental perfusion [17]. Evidence has demonstrated that exposure to CeO_2 nanoparticles can inhibit trophoblast cell migration and invasion, accompanied by abnormal placental development [18]. These findings suggest that cerium exposure may disrupt key biological behaviors of trophoblast cells, thereby impairing the establishment of placental blood perfusion and increasing the risk of fetal growth restriction.Biomonitoring studies have detected cerium in maternal blood and urine, as well as in placental tissue and cord blood, indicating that cerium may cross the placental barrier [19–20]. Mechanistically, cerium exposure can induce oxidative stress and inflammatory responses, disrupt mitochondrial function, and inhibit trophoblast proliferation, invasion, and placental angiogenesis, ultimately impairing placental perfusion and nutrient transport [21–22].

Secreted cytokines have long been recognized as mediators of intercellular communication among different cell types. Increasing evidence indicates that exosomes play an important role in intercellular communication at the maternal-fetal interface. Exosomes refer to those cell secretions having round shape and the size are between 30–150 nm. [23]. There are many kinds of cells, including immune, stem, and cancer cells that secrete exosomes by exocytosis. [24], and these vesicles are widely present in biological fluids such as urine, saliva, blood, and amniotic fluid [25].Exosomes have complex structures and contain abundant macromolecules: Proteins, lipids, DNA including two strands with different RNA species. [26]. These molecules can be transported through body fluids and subsequently internalized by recipient cells, thereby regulating gene expression and cellular functions [27]. Earlier researches show that exosomes derived from bovine endometrial epithelial cell have 254 protein and 227 miRNA and all is associated with trophoblast attachment during embryo implantation. [28]. Similarly, exosomes emitted from human placental cells have about 250 proteins as well as like miR-21 and mira-126 which are also involved in angiogenesis and growth and cell migration.[29]. These exosomes can be taken up by recipient cells through autocrine or paracrine mechanisms [30–31].Therefore, decidua-derived exosomes may regulate trophoblast invasion and help maintain the dynamic balance at the maternal–fetal interface. Placenta-derived exosomes at the maternal–fetal interface can regulate trophoblast function through autocrine signaling and can also be secreted into the maternal circulation to modulate systemic vascular endothelial cells. Consequently, whether prenatal cerium exposure alters the composition of decidua-derived exosomes and subsequently affects trophoblast invasion warrants further investigation.

Therefore, in this study, cerium nitrate ($Ce(NO_3)_3$) was used as the exposure factor to establish a rat model of early gestational exposure to different doses of cerium. The aim is to study the effect of Maternal $Ce(NO_3)_3$ intake on the early stage embryonic development and maternal pregnancy result. We also considered the secretory of decidual which controls trophoblastic entry. And this research, we study cerium intake effect on decidual exosome derived miRna and what happen with the embryo after mother get cerium through cell signaling. These findings may provide experimental evidence for the effective prevention and control of the adverse biological effects associated with cerium exposure.

2. Materials and Methods

2.1 Experimental Animals and Grouping

In this paper the specific pathogen free(SPF)Sprague–Dawley （SD）rats were used., including 9-week-old males weighing (250 ± 10) g and 8-week-old females weighing (230 ± 10) g. All animals were purchased from SPF (Beijing) Biotechnology Co., Ltd. (License No. SCXK (Beijing) 2024-0001).They lived in a place surrounded by barriers inside areas with timing on light and darkness being 12 hours, room temperature at around 22 ± 2C, there was an amount of water content from 50–60%. Gestate Mice quality SPF give them, let them freely use the quality of water. All animal experiments were conducted in accordance with the ARRIVE guidelines and the Guidance on the Operation of the Animals (Scientific Procedures) Act 1986, as well as the EU Directive 2010/63/EU and NIH Guide for the Care and Use of Laboratory Animals.All procedures were approved by the Institutional Animal Care and Use Committee (IACUC) of Baotou Medical College, Baotou, Inner Mongolia, China (Approval No.[2023] 1).The sex of the animals used in the study was mixed, and this was considered in the analysis where appropriate.

After one week of acclimatization, female and male rats were housed together at a ratio of 1:1 at 21:00 each day. The following morning at 07:00, the presence of a vaginal plug was examined, and detection of a plug was designated as gestational day 1 (GD1). To ensure comparability with previous studies, the dosing regimen in this study was determined based on published literature using the same toxic agent in Sprague–Dawley rats [32, 33]. There were totally 40 gestation female rats, and their baseline body weights between all groups were not markedly different(n = 10), which then split to reference group(n = 10)and Ce dosage groups with either 50 (n = 10), 100 (n = 10),or 200(n = 10)..From GD1 to GD17, rats were administered either sterile water (control) or $Ce(NO_3)_3$ at doses of 50, 100, or 200 mg/kg once daily by oral gavage. The administration volume was standardized to 1 mL/100 g body weight per day (equivalent to 10 mL/kg). Doses were selected based on previous studies and environmental relevance. Body Mass was noted and recorded daily prior to administration, and the Oral Dose Volume was adjusted according to the Body Mass that was measured on that specific day. The dosing solutions were prepared in sterile water at concentrations of 5, 10, and 20 mg/mL, respectively, freshly prepared before use. General health status, body weight, and dosing information were monitored and recorded throughout the experiment. For terminal sample collection, rats were anesthetized by intraperitoneal injection of sodium pentobarbital (30 mg/kg). Adequate anesthetic depth was confirmed by the absence of response to noxious stimulation prior to tissue collection. Maternal serum, placental tissues, and offspring samples were then collected and stored at − 80°C for subsequent analyses. At the end of the procedure, rats were euthanized by intraperitoneal injection of an overdose of sodium pentobarbital (250 mg/kg). Animals were continuously monitored until death was confirmed by cessation of spontaneous respiration and heartbeat and absence of the corneal reflex. Cervical dislocation was subsequently performed as a secondary physical method to ensure death. All procedures were approved by the institutional animal care and use committee and conducted in accordance with institutional guidelines for the care and use of laboratory animals.

2.2 Cell Culture and Treatment

Human choriocarcinoma JEG-3 cells were obtained from Procell Life Science & Technology Co., Ltd. (Wuhan, China; Cat. No. CL-0127). Cells were cultured in Minimum Essential Medium (MEM) supplemented with 10% fetal bovine serum (FBS) and 1% penicillin–streptomycin solution (PS).Cells were maintained in a humidified incubator at 37°C with 5% CO_2 and a relative humidity of 70–80%. Cells between passages 4 and 8 were used for all experiments. When cell density got to about 70–80%, we switched out the current growth fluid for fresh medium and then began giving drugs.

2.3 Morphological Measurement of Placenta and Fetuses

The uterus was dissected in a culture dish to obtain placentas and fetuses. After separation, placentas and fetuses were transferred into new disposable culture dishes containing phosphate-buffered saline (PBS). Placentas were rinsed thoroughly with PBS to remove residual blood and then weighed using an electronic balance. Placental diameter was measured with a vernier caliper and recorded.A portion of each placenta was further separated into the fetal and maternal sides, placed into 2 mL EP tubes, immediately frozen in liquid nitrogen, and subsequently stored at − 80°C for further analysis.Fetuses were rinsed with PBS to remove blood and debris, after which body weight was measured using an electronic balance and recorded. Fetal body length was then measured with a vernier caliper and documented.

2.4 Sample Selection and Statistical Unit Definition

Each experimental group initially included 10 pregnant rats. For litter size analysis, three dams were randomly selected from each group, and the number of fetuses per litter was recorded, with each dam treated as one biological replicate. For fetal body weight, fetal body length, SGA-like phenotype, placental weight, and placental diameter, all available fetuses or placentas from all dams in each group were included in the analysis. For ICP-MS and placental IL-6 measurements, three dams were randomly selected from each group, and one placenta was randomly collected from each selected dam for analysis. For histological examination, three placentas were randomly selected from each group for H&E staining.

2.5 Determination of Cerium Concentration by Inductively Coupled Plasma Mass Spectrometry (ICP-MS)

A total of 0.35 mL of rat whole blood was transferred into an 8 mL quartz digestion tube, followed by the addition of 0.5 mL of concentrated nitric acid. For placental samples, 300 mg of decidual tissue and 300 mg of trophoblast tissue were separately placed into 8 mL quartz digestion tubes, to which 1 mL of concentrated nitric acid and 0.3 mL of ultrapure water were added. The samples were allowed to stand for 2 h prior to digestion.

Samples were then subjected to microwave digestion (power 1200 W, pressure 40 bar, nitrogen atmosphere) under the following program: heating from room temperature to 150°C within 5 min, followed by heating to 190°C within 5 min, and maintaining at 190°C for 20 min.

After digestion, 0.4 mL of a mixed internal standard solution containing indium (In, 4 ng/mL) and rhenium (Re, 4 ng/mL) was added, and the final volume was adjusted to 8 mL with ultrapure water. The samples were sealed with film, mixed thoroughly, and then analyzed by ICP-MS.The ICP-MS operating conditions were as follows: nebulizer gas flow rate 0.97 L/min, auxiliary gas flow rate 1.80 L/min, plasma gas flow rate 17.5 L/min, radiofrequency power 1150 W, dwell time 50–100 ms, sample uptake rate 1.1 mL/min, scanning mode of single-point peak hopping, and resolution of 0.7–0.9 amu.

2.6 Histological Examination of Placental Tissue

After dissection from pregnant rats, placental tissues were fixed in 4% paraformaldehyde solution. Then they have been rinse, dehydrated with dec-ethanols (dec), decolored with alc-benzine(x), and finally were embedded in paraffin.Paraffin-embedded tissues were sectioned into 7 μm-thick slices using a microtome and mounted onto glass slides. The sections were dried at 65°C for 4.5 h, followed by deparaffinization in xylene and rehydration through a graded ethanol series. The sections were then stained with hematoxylin and eosin (H&E). And then the changes appeared in those placentas were looked at by an optical microscope and photos was taken.

2.7 Isolation of Exosomes from Placental Tissue and Cell Culture Supernatant

Exosomes were isolated from placental tissues and cell culture supernatants using a differential centrifugation method. Briefly, samples were first thawed at 37°C and transferred into new centrifuge tubes. The samples were initially centrifuged at 2,000 × g for 30 min at 4°C to remove large cellular debris. Then the clear fluid were very carefully pipetted in to another series of new centrifuge vial then spin at 10000 *g for 45min on 4 degrees celcuis again remove most of large vesicle.The resulting supernatant was filtered through a 0.45 μm membrane filter, and the filtrate was collected. Then we took the obtained exosome after ultracentrifugation of 100000X G for 90MIN at 4C: After supernatant was taken out, re-suspend the residue with 10mL of cold 1XPBS and do it again by ultracentrifugation for the second time at 100000xg for 90 minutes at 4 degree Celsius for washing.Following removal of the supernatant, the exosome pellet was resuspended in 100 μL of ice-cold 1× PBS. For characterization, 30 μL of the suspension was used for transmission electron microscopy (TEM), 10 μL was used for particle size analysis, and the remaining exosome suspension was stored at − 80°C until further analysis.

We use Transmission electron microscope (TEM)to observe the exosome’s structure feature: Exosomes. That is to say, 10uL exosome solution were added on copper grid and it was dried up after 1min. The extra bit was whiped off with fillopaper: And then 10ul of Uranyl Acetate was dropped on the Grid for Negative Staining and allowed to sit for a minute. Excessive stain was wiped away with filter paper. Then the grid was left to dry for a few min at RT. The acceleration voltage was 80KV, and it is performed..

The particle size distribution and concentration of exosomes were determined using nanoparticle tracking analysis (NTA). Samples were diluted to an appropriate concentration prior to analysis. Instrument performance was first verified using standard calibration particles, after which exosome

samples were analyzed. The instrument automatically generated data on exosome particle size distribution and concentration.

2.8 Transcriptome Sequencing (RNA-seq)

For transcriptome sequencing, three pregnant rats were randomly selected from both the cerium exposure group and the control group. For each dam, placental tissues from all placentas were collected, and equal portions were pooled to generate one composite sample for sequencing. The samples from the cerium-treated group were labeled RMPE_FT1, RMPE_FT2, and RMPE_FT3, while those from the control group were labeled RMPE_FC1, RMPE_FC2, and RMPE_FC3.Immediately after collection, placental tissues were rapidly frozen in liquid nitrogen and subsequently sent to Biopile Biotechnology Co., Ltd. (China) for total RNA extraction and RNA sequencing analysis.

2.9 Differential Expression Analysis of miRNAs

Raw sequencing data obtained from transcriptome sequencing were subjected to quality control to remove reads containing adaptor sequences, reads with more than 10% unknown nucleotides (N), and reads in which more than 50% of bases had a quality score ≤ Q20. The remaining high-quality reads were retained as clean data for subsequent analysis.Differential expression analysis of miRNAs between the cerium exposure group and the control group was performed using DESeq2 (version 1.34.0) implemented in R (version 4.2.2). After false discovery rate (FDR) correction, miRNAs with $|\log2(\text{FoldChange})| > 1$ and FDR < 0.05 were considered significantly differentially expressed.

2.10 Quantitative Real-Time PCR (qRT-PCR) Analysis

To validate the transcriptome sequencing results, three placental tissue samples were randomly selected from both the cerium-treated group and the control group. Total RNA was extracted using the TransZol Up reagent kit according to the manufacturer’s instructions.Second the isolated rna is turned to CDNA through miRNA first strand cDNA synthesis kit under the following conditions: 5' C for Five Mins and 42C For Sixty Minutes, Then 95C For Threeminutes. The expression pattern of the discovered differently regulated genes was verified through the use of qRT-PCR. The amplification program was as follows: 95°C for 10 min; 40 cycles of 94°C for 10 s and 60°C for 30 s; followed by 95°C for 10 s, 65°C for 60 s, and 97°C for 1 s. Relative gene expression levels were calculated using the $2^{-\Delta\Delta Ct}$ method. The genes analyzed and their corresponding primer sequences are listed in Table 1.

Table 1
Primer sequence information

Gene	Species	upstream primer (5—3)	downstream primer (5—3)
rno-miR-483-3p	Rat	TCACTCCTCTCCTCCCGTCTT	
ALIX	Human	AGCCAAATTGCAGCAGAACAG	GAGATATGTCCACGGTCGGC
Syntenin-1	Human	CTCCAGCCTCATTGGTTGGT	TTCAAAGGGCCTGTCACGAA
Ago2	Human	CGTCCTCTGGGACGACAATC	ATGGCTTCCTTCAGCACTGT
IGF2	Human	GACACCCTCCAGTTCGTCTG	GGGGTAGCACAGTACGTCTC
IGF2	Rat	TTGGCCCTCCTGGAGACATA	GTATCTGGGGAAGTCGTCCG
Mir-483	Human	GGGGAAGACGGGAGGAAAG	AGGAGAGGAGTGAGGAGGCG
Mir-483	Rat	GAGGGGGAAGACGGGAGA	ACAAGACGGGAGGGGAGG
rno-miR-483-3p	Rat	CACTCCTCCCCTCCCGTC	
ARBB2	Human	CTGTGTCTGGGGTGGGGATA	GCCGCACAGAGTTCCTTTTG
ARBB2	Rat	GAGCCCTAACTGCAAGCTCA	TCCAGGTCTTCTCGGCCATA
IL-6	Human	CCGGGAACGAAAGAGAAGCTC	ACCGAAGGCGCTTGTGGAG
IL-6	Rat	AGAGACTTCCAGCCAGTTGC	TGCCATTGCACAACTCTTTTC
hsa-miR-483-3p	Human	TCACTCCTCTCCTCCCGTCTT	

2.11 Target Gene Prediction Analysis

miRNAs primarily regulate gene expression at the post-transcriptional level by binding to complementary sequences in the target mRNA. In this paper, the 3’end untranslated regions (3'UTR) of rat mRNAs are target sequences and miranda prediction program was adopted to identify prospective mRNA target gene of dysregulation microRNA.

2.12 Functional Enrichment Analysis of Differentially Expressed Genes

To explore the potential biological functions of differentially expressed miRNAs, Gene Ontology (GO) and Kyoto Encyclopedia of Genes and Genomes (KEGG) pathway analyses were performed to functionally annotate and identify enriched signaling pathways among the predicted target genes.Based on the statistical significance of the enrichment results (P value), biological processes and signaling pathways potentially associated with prenatal cerium exposure were identified.

2.13 Cell Viability Assay (CCK-8)

Cell viability was assessed using the Cell Counting Kit-8 (CCK-8; Dojindo, Japan). Cells in the logarithmic growth phase were seeded into 96-well plates at equal densities, with 100 µL of culture medium added to each well. After cell attachment, the cells were treated with different concentrations of the test compound (e.g., cerium nitrate solution) for 24 h or 48 h.Afterwards, the amount of CCK − 8 solution which was added to each well is 10µl and then these plates were left in a humidified chamber at 37°C with 5%CO2 for further 1–2 hours. The absorbance at 450 nm (OD450) was then measured using a microplate reader to evaluate cell viability.

2.14 Flow Cytometry Analysis

Cell apoptosis was analyzed using flow cytometry. After treatment, cells from each group were collected, washed twice with phosphate-buffered saline (PBS), and centrifuged to remove the supernatant. The following is how we determined cell apoptosis: We employed AnnexinV-FITC/PI Apoptosis detection kit(BD,Bio-sciences,U.S.A), according to the supplier's guidelines. The sample was diluted with 1x Binding Buffer. Then 5uL Annexin V - FITC was added, also 5uL PI was added.The mixture was incubated for 15 min at room temperature in the dark. Subsequently, fluorescence signals were detected using a flow cytometer (e.g., BD FACSCanto II). The excitation wavelength was set to be 488nm. The proportions of early apoptotic cells (Annexin V^+/PI^-) and late apoptotic cells (Annexin V^+/PI^+) were analyzed.

2.15 Enzyme-Linked Immunosorbent Assay (ELISA)

JEG-3 cells treated with different concentrations of cerium and their corresponding culture media were collected, along with placental tissues from different experimental groups. Concentrations of IL − 6 in the cell culture media, cellular extracts, and placental tissues were measured using a rat IL-6 ELISA kit (Enzyme-linked immunosorbent assay kit, China) according to the manufacturer’s instructions.

2.16 Western Blot Analysis

For the western blots, we got cell lysates for JEG-3 and rat maternal placentas. Cell lysates were prepared using lysis buffer supplemented with a protease inhibitor mixture containing 1 mM PMSF (Beyotime, China), while placental tissues were homogenized in RIPA buffer (Beyotime, China).In order to determine the quantity of protein, the Pierce™BCAProteinAssayKit (Thermo FisherScientific,U.S.A) had been employed according to the manufacturer’s instructions. Equal amounts of protein were separated by SDS–PAGE and subsequently transferred onto polyvinylidene fluoride (PVDF) membranes (Millipore, USA). The membranes were blocked with QuickBlock blocking buffer (Beyotime, China) for 1 h at room temperature.After blocking, the membranes were incubated overnight at 4°C with specific primary antibodies. Following washing, the membranes were incubated with goat anti-rabbit secondary antibodies diluted at 1:50,000 for 1 h at room temperature. Protein bands were detected using an Odyssey CLx infrared imaging system. On Image J was done to check signal ampltiude and normalize with GADPH as referece.

2.17 Statistical Analysis

The statistical evaluations were done by the SPSS programme, version 25. 0. For numerical figures it is expressed as mean ± SD. Two sample group wise contrast is done using independent - samples t- test while comparison among more than 2 groups is done with oneway - anova (one way anova).When the assumption of homogeneity of variance was satisfied, pairwise comparisons between groups were conducted using the Student–Newman–Keuls (SNK-q) test. When the assumption of equal variances was not met, the Games–Howell test was applied. A two-tailed *P* value < 0.05 was considered statistically significant.

3. Results

3.1 Effects of Prenatal Cerium Exposure on Placental and Fetal Growth

Maternal exposure to cerium nitrate during pregnancy produced significant dose-dependent effects on placental and fetal growth. As shown in Figure 1A, different doses of cerium nitrate exposure affected fetal morphology, with the high-dose group (200 mg/kg) exhibiting the most pronounced morphological abnormalities.Figures 1B–E illustrate the effects of cerium exposure on fetal growth parameters. It was discovered that the number of offspring dropped dramatically as dosage of exposure increased; particularly at 100mg/kg and 200mg/kg where there were very few offspring with only 5% (P<.01) or zero offspring(P<.0001) respectively. In addition, gestational body mass was greatly decreased among the high - concentration group(P <0.001 and P < 0.0001) , but there were no considerable changes in neonatal length among all groups..Furthermore, Figure 1E presents the proportion of SGA babies, which is notably larger than in the medium and high dose groups, being more than P<0.05 and P<0.01 respectively, suggesting that prenatal exposure to cerium nitrate may induce fetal growth restriction. Overall, these findings indicate that maternal cerium exposure during pregnancy markedly affects placental and fetal development, particularly at higher exposure levels, resulting in impaired fetal growth and an increased incidence of SGA.Figure 2 illustrates the effects of different doses of cerium nitrate exposure on placental development. Figure 2A shows that as placental mass dropped with more cerium intake, there was an obvious dip for the group who took the most cerium (200 mg/kg) compared to the baseline group (P<0.01and P<0.0001).Figure 2B shows the changes in placental diameter. With increasing exposure doses, placental diameter gradually decreased, and a significant reduction was observed in the high-dose group compared with the control group (*P* < 0.05).Figures 2C and 2D further present the cerium concentrations in the placental decidual region and blood. The results indicate that cerium levels increased significantly in a dose-dependent manner (*P* < 0.0001 and *P* < 0.01).As we can see from Fig. 2E, cerium concentration in placental trophoblast cells was significantly higher than that of the control group in both medium-dose and high-dose groups (P<0.001).

Figure 1. Dose-dependent effects of cerium exposure on fetal development and growth phenotypes prior to delivery.

3.2 Gestational cerium exposure induces placental pathological alterations and inflammatory cell infiltration

As shown in Figure 2F, H&E staining of placental tissues revealed evident structural alterations following gestational cerium nitrate exposure. In the control group, the placental architecture remained intact, with a clear boundary between the labyrinth layer and the spongiotrophoblast layer. Trophoblast cells were orderly arranged, and both cytoplasmic and nuclear morphologies appeared normal. In contrast, the low- and medium-dose groups exhibited mild edema, vascular congestion, and inflammatory cell infiltration in placental tissues. The severity of these pathological changes gradually increased with rising exposure doses. In the high-dose group, pronounced pathological lesions were observed, including trophoblast degeneration, cytoplasmic vacuolization, nuclear pyknosis, and focal hemorrhage. These findings suggest that high-dose cerium nitrate exposure disrupts placental structural integrity and impairs the function of the maternal–fetal interface, potentially contributing to intrauterine growth restriction.

In addition, as illustrated in Figure 2F, IL - 6 concentration in the ceremium treated groups was very high, and there was evident dose - dependent increase.Notably, the 100 mg/kg and 200 mg/kg groups showed statistically significant differences compared with the control group ($P < 0.05$ and $P < 0.01$, respectively), indicating a marked enhancement of the inflammatory response in placental tissues following cerium exposure.

Figure 2: Effects of Different Dose Treatments on the Placenta of Prepartum SD Rats

3.3 Differential expression analysis of placental exosomal miRNAs following cerium exposure

To investigate the effects of gestational cerium exposure on miRNA expression in placental exosomes at the maternal–fetal interface, miRNA sequencing analysis was performed. After false discovery rate (FDR) correction ($|\log_2 FC| > 1$, FDR < 0.05), only one significantly upregulated miRNA was identified, while no significantly downregulated miRNAs were detected (Figure 3A). Overall, the alterations in miRNA expression between the cerium-exposed group and the control group were relatively limited.

3.4 GO and KEGG enrichment analysis of differentially expressed exosomal miRNAs in rat placenta following gestational Ce exposure

To further explore the potential biological functions associated with cerium exposure, Gene Ontology (GO) enrichment analysis was performed on the predicted target genes of the differentially expressed miRNAs. As shown in Figure 3B, in the cellular component (CC) category, the target genes were mainly enriched in extracellular exosomes, cytoplasm, and cytosol. Molecular function(MF): within this MF group, there were some noticeably abundant classifications: phosphoprotein phosphatase activity;protein tyrosine phosphatase activity;oxidoreductase activity. In the biological process (BP) category, the enriched terms were primarily associated with regulation of the cell cycle process, response to steroid hormones, cellular response to chemical stress, and cell proliferation.

Furthermore, We did pathway enrichment by using Kyoto encyclopedia of genes and genomes or KEGG to see which signal network may be involved in the result caused from taking in cerium. As illustrated in Figure 3C, several significantly enriched pathways were identified. Notably, pathways related to

inflammatory responses and cellular stress were prominently enriched, including the MAPK signaling pathway, TNF signaling pathway, FcεRI signaling pathway, and the inflammatory mediator regulation of TRP channels pathway. And also there were considerable enrichments for the AMPK signaling pathway and routes related to choline metabolism and phospholipid signaling.

Figure 3. Differential expression analysis and KEGG pathway enrichment of identified genes.

3.5 Coordinated upregulation of IGF2 and its intronic miR-483-3p in the placenta

To validate the sequencing results, quantitative real-time PCR (qPCR) was performed to measure the expression levels of miR-483-3p in both serum and placental tissues. As seen from figures 4AB, Prenatal cerium intake clearly increased the miR-483 - 3p in concentration manner. Meanwhile, the expression of pri-miR-483 was also markedly elevated (Figure 4C), suggesting that this miRNA may be regulated at the transcriptional level. Since miR-483-3p is within an intronic part of the IGF2 gene we looked at the transcriptional activity of IGF2. The IGF2 mRNA was notably higher in the cerium treated group when compared with the reference group as seen in Figure 4D.

Figure 4. Effects of different doses of cerium exposure on the expression of miR-483 and IGF2 in placental tissues prior to delivery.

3.6 Cell viability assessed by CCK-8 assay

In order to examine the effect of Ce(NO3)3 on trophoblast cell (JEG - 3), CCK - 8 method was employed to count cell viability after a 24 h incubation with different concentrations including 0, 2, 4, 6, 8, 10, and 16 ug/mL. As shown in Figure 5A, cell viability exhibited a clear dose-dependent decrease with increasing concentrations of $Ce(NO_3)_3$. Compared with the control group (0 μg/mL), no significant change in cell viability was observed in the 2 μg/mL treatment group ($P > 0.05$). However, a significant reduction in cell viability was detected starting from 4 μg/mL ($P < 0.05$). At concentrations of 6 μg/mL and above, cell viability declined further, with the most pronounced decreases observed in the 10 μg/mL and 16 μg/mL groups ($P < 0.001$ and $P < 0.0001$, respectively), indicating that high concentrations of $Ce(NO_3)_3$ exert a marked inhibitory effect on trophoblast cell viability.

3.7 Cerium exposure induces apoptosis in trophoblast cells

To evaluate the effect of cerium nitrate on trophoblast cell apoptosis, flow cytometry analysis was performed using Annexin V–FITC/PI double staining (Figures 5B–C). The results showed that the proportion of apoptotic cells increased in a dose-dependent manner with increasing concentrations of cerium nitrate. Compared with the blank group, which exhibited an apoptosis rate of 14.1%, the apoptosis rates in the 2 μM, 4 μM, and 8 μM treatment groups increased to 21.5%, 36.6%, and 38.7%, respectively. Statistical analysis indicated that the apoptosis rates in all treatment groups were significantly higher than those in the control group ($P < 0.0001$). These findings suggest that cerium nitrate induces apoptosis in trophoblast cells, which may represent an important mechanism underlying cerium-induced placental dysfunction and fetal growth restriction.

3.8 Cerium exposure activates inflammatory responses and the IGF2/miR-483 locus in trophoblast cells

Cerium treatment significantly increased IL-6 expression in JEG-3 cells in a dose-dependent manner (Figures 5D–E), indicating activation of inflammatory signaling pathways. In addition, the expression of **IGF2** mRNA was markedly elevated (Figure 5G). Consistently, the expression levels of mature **miR-483-3p** (Figure 5F) and its primary transcript **pri-miR-483** (Figure 5H) were also significantly upregulated. Notably, these in vitro findings are consistent with the expression patterns observed in placental tissues, suggesting that cerium exposure may activate the **IGF2/miR-483 locus** and promote inflammatory responses in trophoblast cells.

Figure 5. Effects of cerium on JEG-3 cell viability, apoptosis, and miR-483/IGF2 expression.

3.9 Cerium exposure promotes exosomal secretion of miR-483-3p from trophoblast cells

Exosomes were isolated from the culture supernatant of trophoblast cells following cerium treatment. Transmission electron microscopy revealed the presence of typical cup-shaped vesicular structures characteristic of exosomes (Figure 6A). Nanoparticle tracking analysis showed that the particle size distribution was consistent with the typical size range of exosomes (Figure 6B). Western blot analysis further confirmed the successful isolation of exosomes, as the exosomal markers CD9, CD63, CD81, and TSG101 were positively expressed, whereas the Golgi marker GM130 was not detected (Figure 6C).

Further analysis demonstrated that cerium exposure significantly increased the level of miR-483-3p in exosomes in a dose-dependent manner (Figure 6D). In addition, the expression levels of proteins associated with exosome biogenesis and RNA loading, including ALIX, Ago2, and Sytenin-1, were significantly upregulated (Figures 6E–G). These results indicate that cerium exposure enhances the miRNA packaging process and promotes the secretion of miR-483-3p via exosomes. This exosome-mediated transfer of miR-483-3p may facilitate intercellular communication and signaling during placental inflammatory responses.

Figure 6. Cerium exposure promotes exosome-mediated secretion of miR-483-3p in trophoblast cells.

3.10 Gestational cerium exposure may increase the risk of SGA by activating the MAPK signaling pathway and promoting placental dysfunction

Is MAPK signaling cascade involved in Ce mediated inflammatory response? We checked out the phosphorylation status of p38. In trophoblast cells, cerium treatment markedly increased the expression of phosphorylated P38 (p-P38) in a dose-dependent manner, whereas the expression of total P38 remained unchanged (Figures 7A–C). Quantitative analysis further demonstrated a significant increase in the p-P38/P38 ratio. The same result was found about the placentas from experiment animals: the p-P38 level is a great deal larger when the Cerium has been used, contrary to the reference, while the total P38 protein level showed no significant difference (Figures 7D–F).These findings indicate that cerium exposure activates the MAPK/P38 signaling pathway both in vivo and in vitro, suggesting that P38

phosphorylation may play a critical role in cerium-induced placental inflammatory responses and subsequent placental dysfunction.

Figure 7. Cerium exposure activates the MAPK signaling pathway.

4. Discussion

In recent years, Ce, a commonly used light rare earth element, has attracted increasing attention due to its growing environmental presence and potential toxicological effects, particularly on pregnant women and fetal development [34]. Emerging evidence suggests that cerium exposure may exert adverse effects on fetal growth and development. Notably, elevated exposure during pregnancy has been associated with an increased risk of SGA infants [35]. Although several studies have explored the impact of cerium on fetal development, the underlying mechanisms and its specific association with the occurrence of SGA remain incompletely understood. Previous research by Zhong et al. demonstrated that cerium exposure leads to abnormal placental blood sinus structures and reduced trophoblast invasion in mice, suggesting that Ce may disrupt normal fetal development by affecting placental angiogenesis and trophoblast function [36]. Other studies have reported that Ce exposure significantly reduces the area of the placental labyrinth layer, induces placental structural damage, and impairs trophoblast invasive capacity, indicating pronounced placental toxicity associated with cerium exposure [37]. These findings are consistent with the results observed in the present study.

Our study demonstrated that Ce accumulation was accompanied by damage to the placental labyrinth zone and functional alterations in trophoblast cells, which may be closely associated with local inflammatory responses, particularly the upregulation of IL-6. Previous studies have reported that the accumulation of Ce in tissues can induce oxidative stress and activate signaling pathways such as NF-κB and MAPK, leading to increased expression of pro-inflammatory cytokines and the initiation of inflammatory cascade reactions [38]. In addition, previous studies have shown that Ce exposure in trophoblast cells is associated with increased expression of IL-6 and IL-8, as well as activation of the NF-κB pathway, which are indicative of inflammatory responses [39]. Furthermore, although IL-6 plays an important role in regulating trophoblast function and angiogenesis during normal pregnancy, its pathological overexpression may inhibit trophoblast invasion and disrupt placental homeostasis [40].

Based on previous acute toxicity assessments, a subchronic toxicity study in rats demonstrated that the no-observed-adverse-effect level (NOAEL) of mixed rare earth nitrates was 200 mg/kg[41]. Wu et al. [42]reported that oral exposure to cerium nitrate at a dose of 300 mg/(kg·d) for 90 days resulted in a significant reduction in body weight in male rats, along with abnormalities in certain hematological and biochemical parameters in the medium- and high-dose groups. Their findings further suggested that oral exposure to cerium nitrate at doses below 75 mg/(kg·d) may not induce observable adverse effects in rats[43]. Therefore, 200 mg/kg was selected as the highest exposure dose in the present study.

Exosomes are nanoscale extracellular vesicles secreted by cells that carry a variety of bioactive molecules, including proteins, RNAs, and lipids, and play important roles in intercellular communication

[44]. During placental development, exosomes are critical regulators of trophoblast cell function [45]. By transferring molecular signals such as miRNAs and mRNAs, exosomes can modulate placental growth, angiogenesis, and immune responses, thereby influencing fetal development [46]. Previous studies have suggested that Ce exposure may alter the composition of placental exosomes, particularly the expression profiles of miRNAs, thereby affecting trophoblast cell function [47]. Moreover, exosome-associated miRNAs have been shown to regulate trophoblast invasion and differentiation capacity [48], which may represent a potential mechanism underlying Ce-induced placental injury. In the present study, we found that Ce exposure significantly altered the level of miR-483-3p in placental exosomes, suggesting that cerium may contribute to placental inflammatory responses and trophoblast dysfunction through miRNA-mediated regulatory mechanisms.

miR-483-3p is located within the IGF2 gene and is co-expressed with its host gene. IGF2 is a key regulator of placental development and fetal growth [49]. From prior study we can see that miR-483-3p being up-regulated reduces IGF1 due to focusing on the IGF1 transcript and stopping it from translating, thereby leading to fetal growth restriction [50]. Although placental function may remain relatively preserved, the reduction in IGF1 results in significant impairment of fetal growth. In transgenic mouse models, overexpression of miR-483-3p has been shown to cause fetal growth restriction accompanied by cardiovascular defects during mid-gestation. Specifically, fetal body weight was reduced by approximately 58% at mid-gestation, indicating that miR-483-3p overexpression markedly inhibits fetal growth and contributes to reduced fetal weight and cardiovascular abnormalities [51]. During fetal development, IGF2 promotes fetal growth by regulating cellular proliferation and metabolic activity, particularly during early embryonic development [52]. Furthermore, IGF2 supports intrauterine fetal development by stimulating fetal growth signals and enhancing the transport of nutrients across the placenta [53]. Altered expression of IGF2 and miR-483-3p may be relevant to placental dysfunction and fetal growth impairment[54].

The present study suggests that cerium exposure is associated with placental inflammatory responses, trophoblast dysfunction, and altered exosomal miR-483-3p expression.In line with previous studies showing that miR – 483–3p is an important controller of placental function, embryogenesis, and the uterine immune response.

In summary, the present study suggests that gestational Ce exposure may induce placental dysfunction and contribute to fetal growth restriction, potentially through disrupting placental structure, inhibiting trophoblast cell viability, and perturbing the regulatory network of exosomal miRNAs. These findings are consistent with previous studies linking environmental exposures to placental abnormalities and increased risk of SGA. Moreover, our results provide preliminary evidence and potential mechanistic clues of rare earth element exposure on adverse pregnancy outcomes. Notably, exosomal miR-483-3p may represent a potential biomarker candidate for assessing Ce exposure risk and warrants further investigation, rather than immediate clinical application.

Several limitations should be acknowledged. First, this study was based on a rat model and a trophoblast-derived cell line, and caution is required when extrapolating the findings to human pregnancy. Second, JEG-3 cells are derived from choriocarcinoma and may not fully recapitulate the biological behavior of primary trophoblasts. Third, although we observed concurrent changes in p38 MAPK activation, IGF2/miR-483-3p expression, and exosomal miR-483-3p release, we did not perform mechanistic intervention experiments, such as pathway inhibition or miRNA gain-/loss-of-function assays, to establish causality. Fourth, the RNA-seq analysis was conducted on a limited number of samples, and the biomarker potential of exosomal miR-483-3p was not validated in maternal circulation or external cohorts. Finally, the exposure doses used in the animal model may not directly reflect real-world human exposure levels, which should be considered when interpreting the translational relevance of the findings.

Declarations

Acknowledgements: We would like to acknowledge Jinlei Du and Lailai Yan for their data collection. We also appreciate the contributions of Rui Qiao and Dapeng Tai for experimental guidance.

Author Contributions: Conceptualization: Jinlei Du and Dapeng Tai; Data curation: Zitong Wang; Formal analysis: Jianhua Cao; Funding acquisition: Rui Qiao and Dapeng Tai; Investigation:Lailai Yan;Methodology: Shuai Li and Yu Qiao; Project administration: Dapeng Tai; Resources: Lailai Yan and Rui Qiao; Software: Lan Luo and Qi Zhang; Supervision:Dapeng Tai; Validation: Jinlei Du and Lailai Yan ; Visualization: Lailai Yan ; Writing – original draft: Jinlei Du; Writing – review and editing:Rui Qiao and Dapeng Tai

Funding: This work was supported by grants from National Natural Science Foundation of China (82060600); Inner Mongolia Autonomous Region Higher Education "Youth Technology Mentorship Support Program"(NJYT23025);Baotou medical college research projects for cultivation of public health and preventive medicine first-class discipline(GWGG-20250801);Baotou Medical College 2026 Bud Program;Baotou Medical College 2026 Undergraduate Innovation and Entrepreneurship Training Program;Baotou Medical College 2025 Bud Program□110-2025300812 □

Disclosing the use of generative AI and AI-assisted technologies during the writing process

During the preparation of this work, the author used ChatGPT to check for grammatical errors and improve sentence structure in the “Introduction” and “Discussion” sections. After using this tool, the author reviewed and edited the content as necessary and assumes full responsibility for the content of the publication.

Conflicts of Interest: The authors declare no conflicts of interest.

Clinical trial registration number: Not applicable.

References

1. Cerium – an overview ScienceDirect Topics. Elsevier. Accessed February 24, 2026. Available at: https://www.sciencedirect.com/topics/materials-science/cerium
2. Lazareva PI, Stupin VA, Lazarev KA, Litvitskiy PF, Manturova NE, Silina EV (2025) Biodistribution and Toxicological Impact Assessment of Cerium Dioxide Nanoparticles in Murine Models: A Systematic Review of In Vivo and Ex Vivo Studies. Pharmaceutics 17(11):1475. 10.3390/pharmaceutics17111475
3. A Two-Generation Reproductive Toxicity Study of Cerium (2026) Springer Accessed Febr 24. 10.1007/s12011-023-03692-2
4. Ren L, Shi W, Tian Y et al (2024) A Two-Generation Reproductive Toxicity Study of Cerium Nitrate in Sprague-Dawley Rats. Biol Trace Elem Res 202(2):597–614. 10.1007/s12011-023-03692-2
5. Casals E, Zeng M, Parra-Robert M et al (2020) Cerium Oxide Nanoparticles: Advances in Biodistribution, Toxicity, and Preclinical Exploration. Small 16(20):e1907322. 10.1002/smll.201907322
6. Ma J, Tian Y, Du C et al (2025) Cerium-doped Prussian blue biomimetic nanozyme as an amplified pyroptosis inhibitor mitigate Aβ oligomer-induced neurotoxicity in Alzheimer's disease. J Nanobiotechnol 23(1):181 Published 2025 Mar 6. 10.1186/s12951-025-03263-8
7. Wang Y, He L, Dong S et al (2023) Accumulation, translocation, and fractionation of rare earth elements (REEs) in fern species of hyperaccumulators and non-hyperaccumulators growing in urban areas. Sci Total Environ 905:167344. 10.1016/j.scitotenv.2023.167344
8. Dai L, Wang L, Wan X et al (2022) Potentially toxic elements exposure biomonitoring in the elderly around the largest polymetallic rare earth ore mining and smelting area in China. Sci Total Environ 853:158635. 10.1016/j.scitotenv.2022.158635
9. Wang S, Li J, Wu Y, Liu X, Zhang L (2025) Modifying effects of prenatal exposure to rare earth elements on birth outcomes through maternal thyroid function in early pregnancy. Environ Pollut 366:125507. 10.1016/j.envpol.2024.125507
10. Wang S, Li J, Wu Y, Liu X, Zhang L (2025) Modifying effects of prenatal exposure to rare earth elements on birth outcomes through maternal thyroid function in early pregnancy. Environ Pollut 366:125507. 10.1016/j.envpol.2024.125507
11. Gordijn SJ, Beune IM, Thilaganathan B et al (2016) Consensus definition of fetal growth restriction: a Delphi procedure. Ultrasound Obstet Gynecol 48(3):333–339. 10.1002/uog.15884
12. Morley R, Fewtrell MS, Abbott RA, Stephenson T, MacFadyen U, Lucas A (2004) Neurodevelopment in children born small for gestational age: a randomized trial of nutrient-enriched versus standard formula and comparison with a reference breastfed group. Pediatrics 113(3 Pt 1):515–521. 10.1542/peds.113.3.515
13. Barker DJ (1995) Fetal origins of coronary heart disease. BMJ 311(6998):171–174. 10.1136/bmj.311.6998.171

14. Vrijheid M, Casas M, Gascon M, Valvi D, Nieuwenhuijsen M (2016) Environmental pollutants and child health-A review of recent concerns. Int J Hyg Environ Health 219(4–5):331–342. 10.1016/j.ijheh.2016.05.001
15. Burton GJ, Fowden AL (2015) The placenta: a multifaceted, transient organ. Philos Trans R Soc Lond B Biol Sci 370(1663):20140066. 10.1098/rstb.2014.0066
16. Deval G, Boland S, Fournier T, Ferecatu I (2021) On Placental Toxicology Studies and Cerium Dioxide Nanoparticles. Int J Mol Sci 22(22):12266 Published 2021 Nov 12. 10.3390/ijms222212266
17. Pijnenborg R, Vercruysse L, Hanssens M (2006) The uterine spiral arteries in human pregnancy: facts and controversies. Placenta 27(9–10):939–958. 10.1016/j.placenta.2005.12.006
18. Zhong H, Geng Y, Chen J et al (2020) Maternal exposure to CeO2NPs during early pregnancy impairs pregnancy by inducing placental abnormalities. J Hazard Mater 389:121830. 10.1016/j.jhazmat.2019.121830
19. Liu Y, Song L, Wu M et al (2023) Association between rare earth element exposure during pregnancy and newborn telomere length. Environ Sci Pollut Res Int 30(13):38751–38760. 10.1007/s11356-022-24958-7
20. Xu X, Wang Y, Han N et al (2021) Early Pregnancy Exposure to Rare Earth Elements and Risk of Gestational Diabetes Mellitus: A Nested Case-Control Study. Front Endocrinol (Lausanne) 12:774142 Published 2021 Dec 20. 10.3389/fendo.2021.774142
21. Chen Z, Zheng M, Wan T et al (2025) Gestational exposure to nanoplastics disrupts fetal development by promoting the placental aging via ferroptosis of syncytiotrophoblast. Environ Int 197:109361. 10.1016/j.envint.2025.109361
22. Yu S, Mu Y, Wang K et al (2024) Gestational exposure to 1-NP induces ferroptosis in placental trophoblasts via CYP1B1/ERK signaling pathway leading to fetal growth restriction. Chem Biol Interact 387:110812. 10.1016/j.cbi.2023.110812
23. Théry C, Zitvogel L, Amigorena S (2002) Exosomes: composition, biogenesis and function. Nat Rev Immunol 2(8):569–579. 10.1038/nri855
24. Kalluri R, LeBleu VS (2020) The biology, function, and biomedical applications of exosomes. Science 367(6478):eaau6977. 10.1126/science.aau6977
25. Raposo G, Stoorvogel W (2013) Extracellular vesicles: exosomes, microvesicles, and friends. J Cell Biol 200(4):373–383. 10.1083/jcb.201211138
26. Thakur BK, Zhang H, Becker A et al (2014) Double-stranded DNA in exosomes: a novel biomarker in cancer detection. Cell Res 24(6):766–769. 10.1038/cr.2014.44
27. Valadi H, Ekström K, Bossios A, Sjöstrand M, Lee JJ, Lötvall JO (2007) Exosome-mediated transfer of mRNAs and microRNAs is a novel mechanism of genetic exchange between cells. Nat Cell Biol 9(6):654–659. 10.1038/ncb1596
28. Burns G, Brooks K, Wildung M, Navakanitworakul R, Christenson LK, Spencer TE (2014) Extracellular vesicles in luminal fluid of the ovine uterus. PLoS ONE 9(3):e90913 Published 2014 Mar 10. 10.1371/journal.pone.0090913

29. Xu P, Ma Y, Wu H, Wang YL (2021) Placenta-Derived MicroRNAs in the Pathophysiology of Human Pregnancy. Front Cell Dev Biol 9:646326 Published 2021 Mar 11. 10.3389/fcell.2021.646326
30. Whiteside TL (2016) Exosomes and tumor-mediated immune suppression. J Clin Invest 126(4):1216–1223. 10.1172/JCI81136
31. Tannetta D, Masliukaite I, Vatish M, Redman C, Sargent I (2017) Update of syncytiotrophoblast derived extracellular vesicles in normal pregnancy and preeclampsia. J Reprod Immunol 119:98–106. 10.1016/j.jri.2016.08.008
32. Ren L, Shi W, Tian Y et al (2024) A Two-Generation Reproductive Toxicity Study of Cerium Nitrate in Sprague-Dawley Rats. Biol Trace Elem Res 202(2):597–614. 10.1007/s12011-023-03692-2
33. Wu Y, Tang X, Yang W et al (2019) Subchronic toxicity of cerium nitrate by 90-day oral exposure in wistar rats. Regul Toxicol Pharmacol 108:104474. 10.1016/j.yrtph.2019.104474
34. Pagano G, Aliberti F, Guida M et al (2015) Rare earth elements in human and animal health: State of art and research priorities. Environ Res 142:215–220. 10.1016/j.envres.2015.06.039
35. Fang X, Xie Y, Cao S et al (2024) Associations between maternal urinary rare earth elements during pregnancy and birth weight-for-gestational age: Roles of cord blood vitamin D levels. Sci Total Environ 912:169222. 10.1016/j.scitotenv.2023.169222
36. Zhong H, Geng Y, Chen J et al (2020) Maternal exposure to CeO2NPs during early pregnancy impairs pregnancy by inducing placental abnormalities. J Hazard Mater 389:121830. 10.1016/j.jhazmat.2019.121830
37. Zhou H, Zhao C, Wang P, Yang W, Zhu H, Zhang S (2023) Regulators involved in trophoblast syncytialization in the placenta of intrauterine growth restriction. Front Endocrinol (Lausanne) 14:1107182 Published 2023 Jan 31. 10.3389/fendo.2023.1107182
38. Park EJ, Choi J, Park YK, Park K (2008) Oxidative stress induced by cerium oxide nanoparticles in cultured BEAS-2B cells. Toxicology 245(1–2):90–100. 10.1016/j.tox.2007.12.022
39. Ma JY, Zhao H, Mercer RR et al (2011) Cerium oxide nanoparticle-induced pulmonary inflammation and alveolar macrophage functional change in rats. Nanotoxicology 5(3):312–325. 10.3109/17435390.2010.519835
40. Jovanović M, Vićovac L (2009) Interleukin-6 stimulates cell migration, invasion and integrin expression in HTR-8/SVneo cell line. Placenta 30(4):320–328. 10.1016/j.placenta.2009.01.013
41. Ji Yunjing L, Jianlin L, Hua HY, Laiyu L, Chaopei H, Wengui X, Yang Jiefang (1987) A Study on the Toxicity of Mixed Rare Earth Elements in Rhesus Monkeys and Their Absorption, Distribution, and Excretion. J Health Toxicol 1(1):8–11
42. WU Y,TANG X Q,YANG W, X et al (2019) Subchronic toxicity of cerium nitrate by 90-day oral exposure in wistar rats[J]. Regul Toxicol Pharmacol 108:104474
43. Liu Jianxin M, Yuhong HW, Carcinogenesis (2022) Teratogenesis Mutagen 34(02):81–87
44. Chen YF, Luh F, Ho YS, Yen Y (2024) Exosomes: a review of biologic function, diagnostic and targeted therapy applications, and clinical trials. J Biomed Sci 31(1):67 Published 2024 Jul 11.

10.1186/s12929-024-01055-0

45. Bai K, Li X, Guo Y et al (2025) The regulatory role of placental extracellular vesicle on trophoblast and endothelial cell functions. Front Cell Dev Biol 13:1528714 Published 2025 Feb 10. 10.3389/fcell.2025.1528714
46. Mitchell MD, Peiris HN, Kobayashi M et al (2015) Placental exosomes in normal and complicated pregnancy. Am J Obstet Gynecol 213(4 Suppl):S173–S181. 10.1016/j.ajog.2015.07.001
47. Freedman AN, Roell K, Engwall E et al (2023) Prenatal Metal Exposure Alters the Placental Proteome in a Sex-Dependent Manner in Extremely Low Gestational Age Newborns: Links to Gestational Age. Int J Mol Sci 24(19):14977 Published 2023 Oct 7. 10.3390/ijms241914977
48. Zhong H, Geng Y, Gao R et al (2023) Decidual derived exosomal miR-99a-5p targets Ppp2r5a to inhibit trophoblast invasion in response to CeO2NPs exposure. Part Fibre Toxicol 20(1):14 Published 2023 Apr 20. 10.1186/s12989-023-00524-y
49. Veronese A, Lupini L, Consiglio J et al (2010) Oncogenic role of miR-483-3p at the IGF2/483 locus. Cancer Res 70(8):3140–3149. 10.1158/0008-5472
50. Wang Y, Hou L, Yuan X et al (2020) miR-483-3p promotes cell proliferation and suppresses apoptosis in rheumatoid arthritis fibroblast-like synoviocytes by targeting IGF-1. Biomed Pharmacother 130:110519. 10.1016/j.biopha.2020.110519
51. Sandovici I, Fernandez-Twinn DS, Campbell N et al (2024) Overexpression of Igf2-derived Mir483 inhibits Igf1 expression and leads to developmental growth restriction and metabolic dysfunction in mice. Cell Rep 43(9):114750. 10.1016/j.celrep.2024.114750
52. DeChiara TM, Robertson EJ, Efstratiadis A (1991) Parental imprinting of the mouse insulin-like growth factor II gene. Cell 64(4):849–859. 10.1016/0092-8674(91)90513-x
53. Sferruzzi-Perri AN, Owens JA, Pringle KG, Roberts CT (2011) The neglected role of insulin-like growth factors in the maternal circulation regulating fetal growth. J Physiol 589(Pt 1):7–20. 10.1113/jphysiol.2010.198622
54. Aykroyd BRL, Tunster SJ, Sferruzzi-Perri AN (2022) Loss of imprinting of the Igf2-H19 ICR1 enhances placental endocrine capacity via sex-specific alterations in signalling pathways in the mouse. Development 149(1):dev199811. 10.1242/dev.199811

Figures

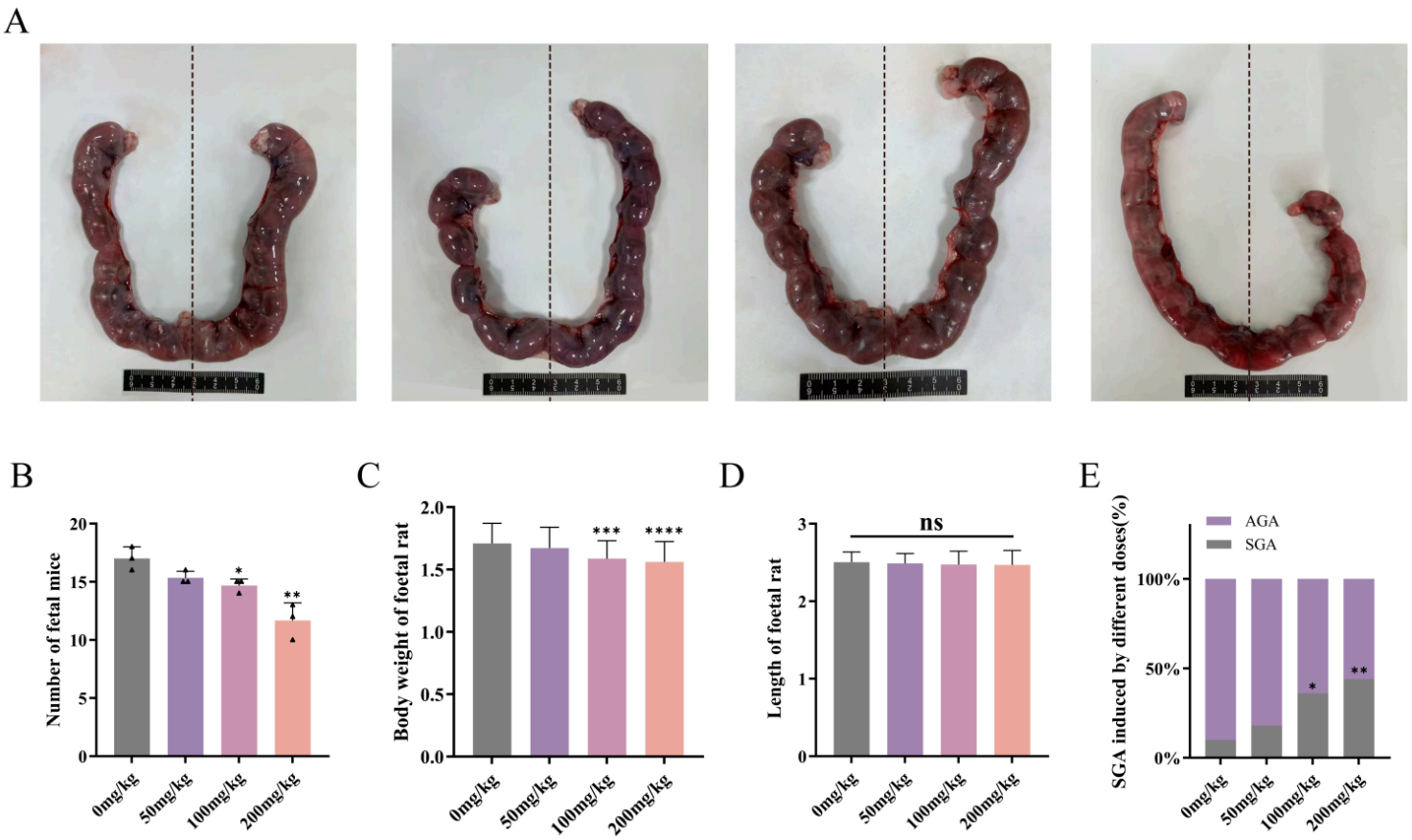


Figure 1

Dose-dependent effects of cerium exposure on fetal development and growth phenotypes prior to delivery. A Uterine Characteristics in Rats at Different Doses B Number of pups C-D Weight and length of baby mice E Incidence of SGA in Fetal Mice Treated with Different Doses of a Toxicant.Data are presented as mean ± SD of three independent experiments.* p 0.05 ** p 0.01 ***p 0.001 ****p 0.0001

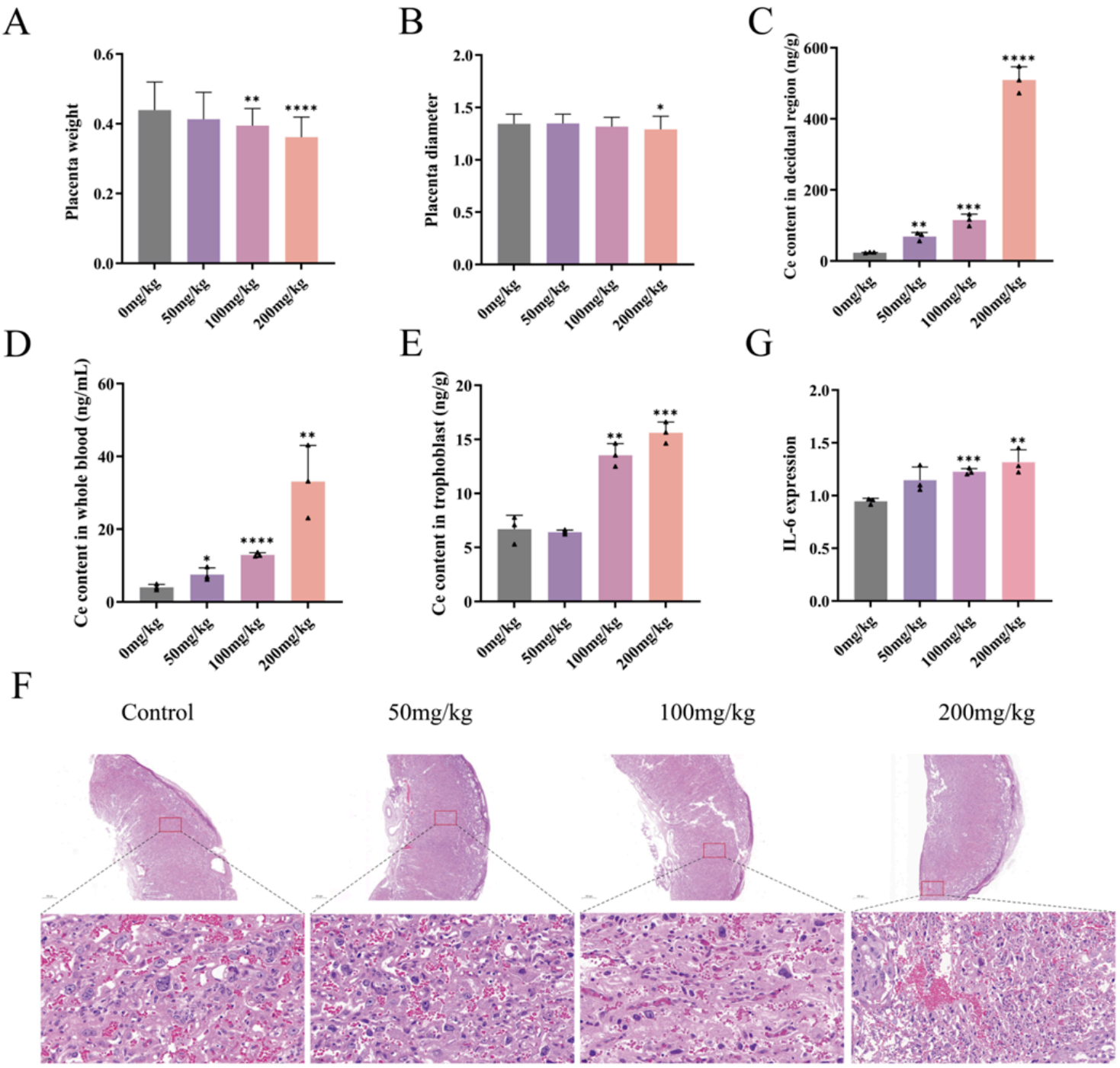


Figure 2

Effects of Different Dose Treatments on the Placenta of Prepartum SD Rats. (A-B)Measure the weight and diameter of the placenta （C-E）Determination of Ce Content Using Inductively Coupled Plasma Mass Spectrometry （D）HE staining to observe histopathological changes. Scale bar = 500 μm / Scale bar = 20 μm（E）IL-6 expression

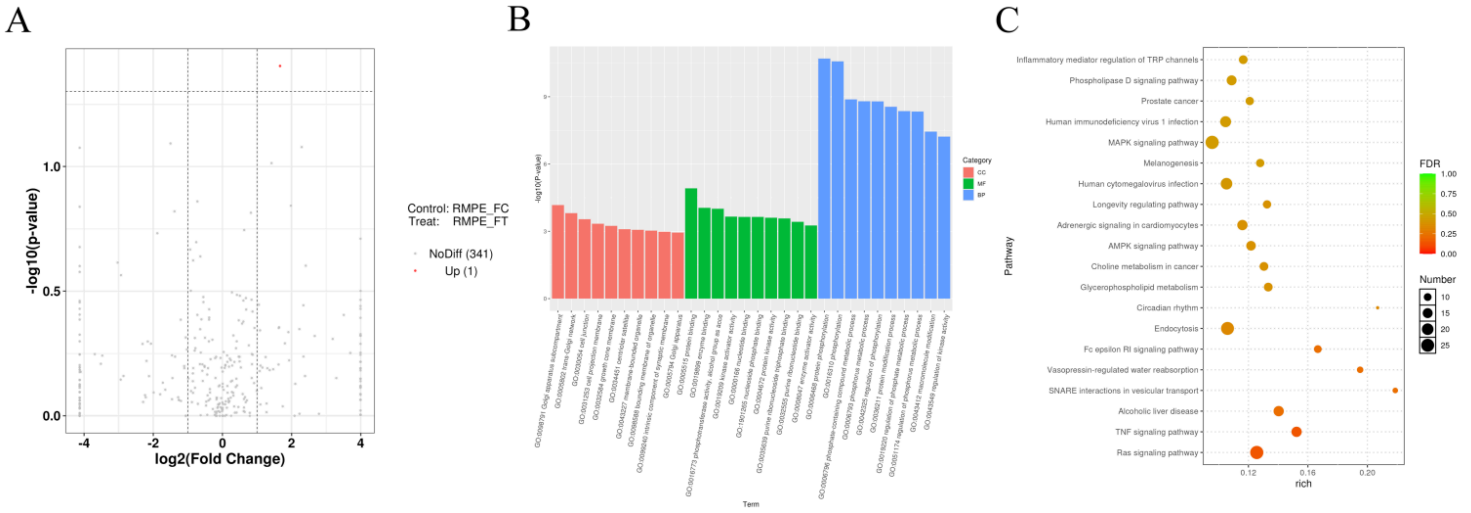


Figure 3

Differential expression analysis and KEGG pathway enrichment of identified genes. （A）Differential Expression of miRNAs in Placental Trophoblast Exosomes RMPE_FC: Exosomes from the decidual zone of the control group placenta RMPE_FT: Exosomes from the decidual zone of the experimental group placenta（B）GO Enrichment Analysis Bar Chart (C) KEGG Enrichment Analysis Scatter Plot

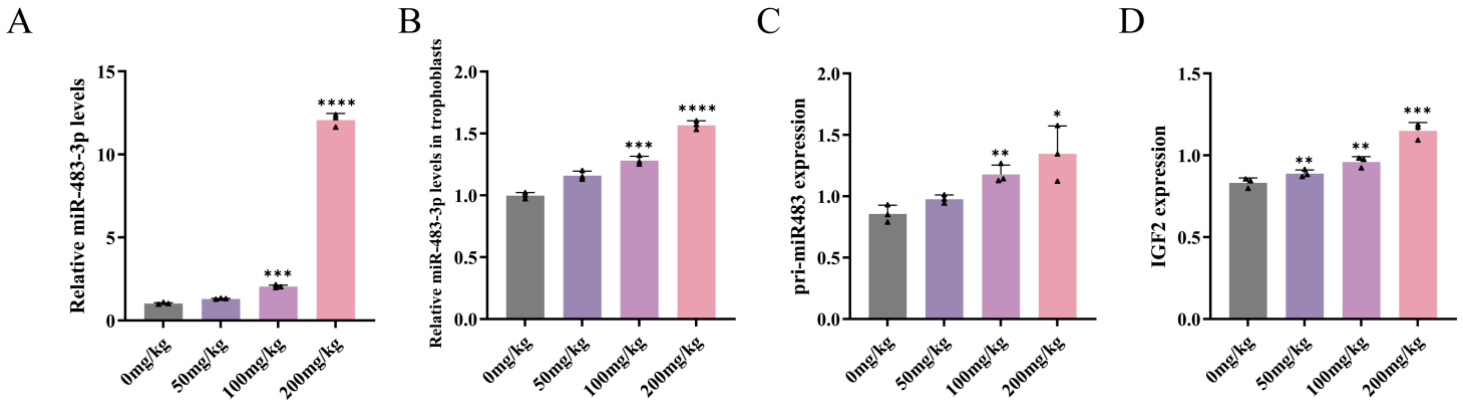


Figure 4

Effects of different doses of cerium exposure on the expression of miR-483 and IGF2 in placental tissues prior to delivery. (A) miR-483-3p expression levels in serum (B) miR-483-3p expression levels in the trophoblast layer of the placenta (C-D) pri-miR-483 and IGF2 gene expression（IGF2 is a key factor in fetal growth and development, playing a role in placental development, cell proliferation, and metabolic regulation.pri-miR-483 is the primary transcript of miR-483-3p, located within an intron of the IGF2 gene. Data are presented as mean ± SD of three independent experiments. * p 〈0.05〉** p〈0.01〉***p〈0.001〉 ****p〈0.0001

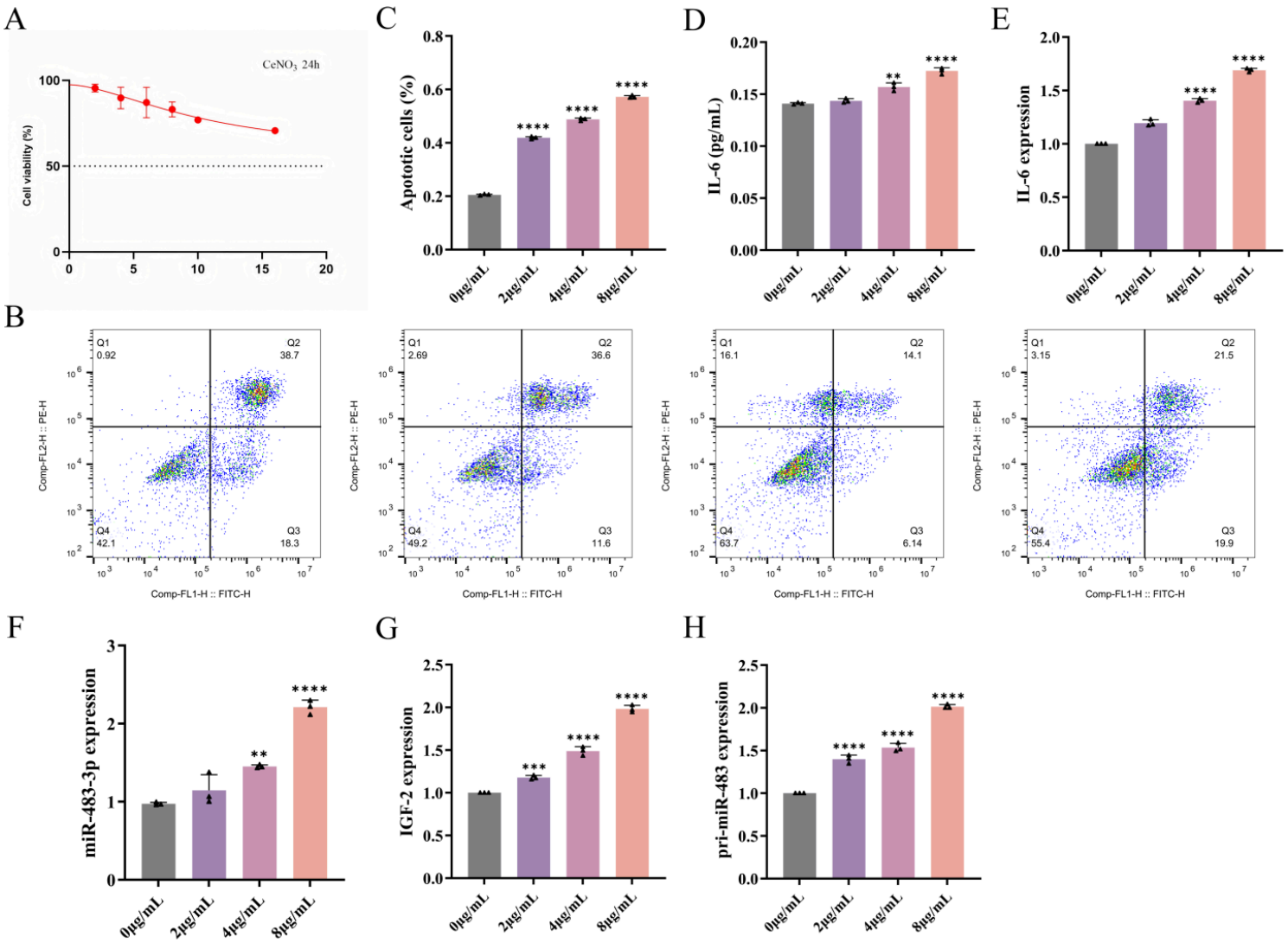


Figure 5

Effects of cerium on JEG-3 cell viability, apoptosis, and miR-483/IGF2 expression. (A) Cell viability after 24 h treatment with increasing concentrations of $Ce(NO_3)_3$, measured by CCK-8 assay. Data are expressed as mean ± SD (n = 3).(B) Representative flow cytometry plots showing apoptosis in JEG-3 cells treated with 0, 2, 4, or 8 μg/mL $Ce(NO_3)_3$ for 24 h. Q2 indicates early apoptotic cells.(C) Quantification of apoptotic cells from flow cytometry.(D–E) IL-6 expression in JEG-3 cells detected by qPCR (D) and ELISA (E) following $Ce(NO_3)_3$ exposure.(F–H) Relative expression levels of miR-483-3p (F), IGF2 (G), and pri-miR-483 (H) measured by qPCR after $Ce(NO_3)_3$ treatment.Data are presented as mean ± SD of three independent experiments. **p < 0.01, ***p□0.001□****p < 0.0001

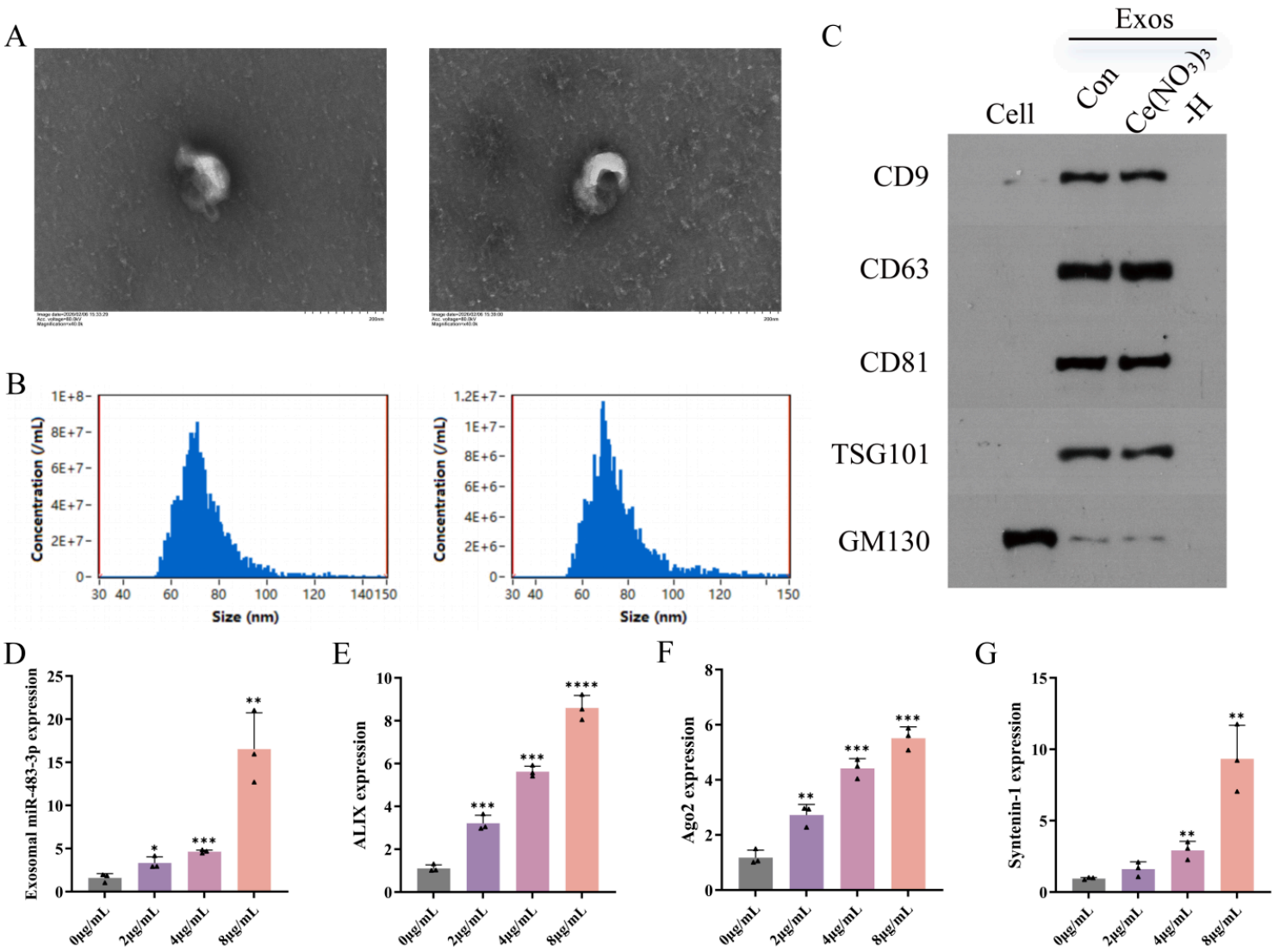


Figure 6

Cerium exposure promotes exosome-mediated secretion of miR-483-3p in trophoblast cells.(A) Representative transmission electron microscopy (TEM) images of exosomes isolated from control and $Ce(NO_3)_3$-treated (8 μg/mL, 24 h) cells. Scale bar = 100 nm.(B) Nanoparticle tracking analysis (NTA) showing size distribution of exosomes from control and $Ce(NO_3)_3$-treated cells.(C) Western blot analysis of exosome markers (CD9, CD63, CD81, TSG101, and GM130) in cells and isolated exosomes.(D–G) Quantification of exosomal miR-483-3p (D) and relative expression of exosome biogenesis-related proteins ALIX (E), Ago2 (F), and Sytenin-1 (G) in JEG-3 cells treated with 0, 2, 4, or 8 μg/mL $Ce(NO_3)_3$ for 24 h.Data represent mean ± SD of three independent experiments. **p < 0.01, ***p < 0.001, ****p < 0.0001.

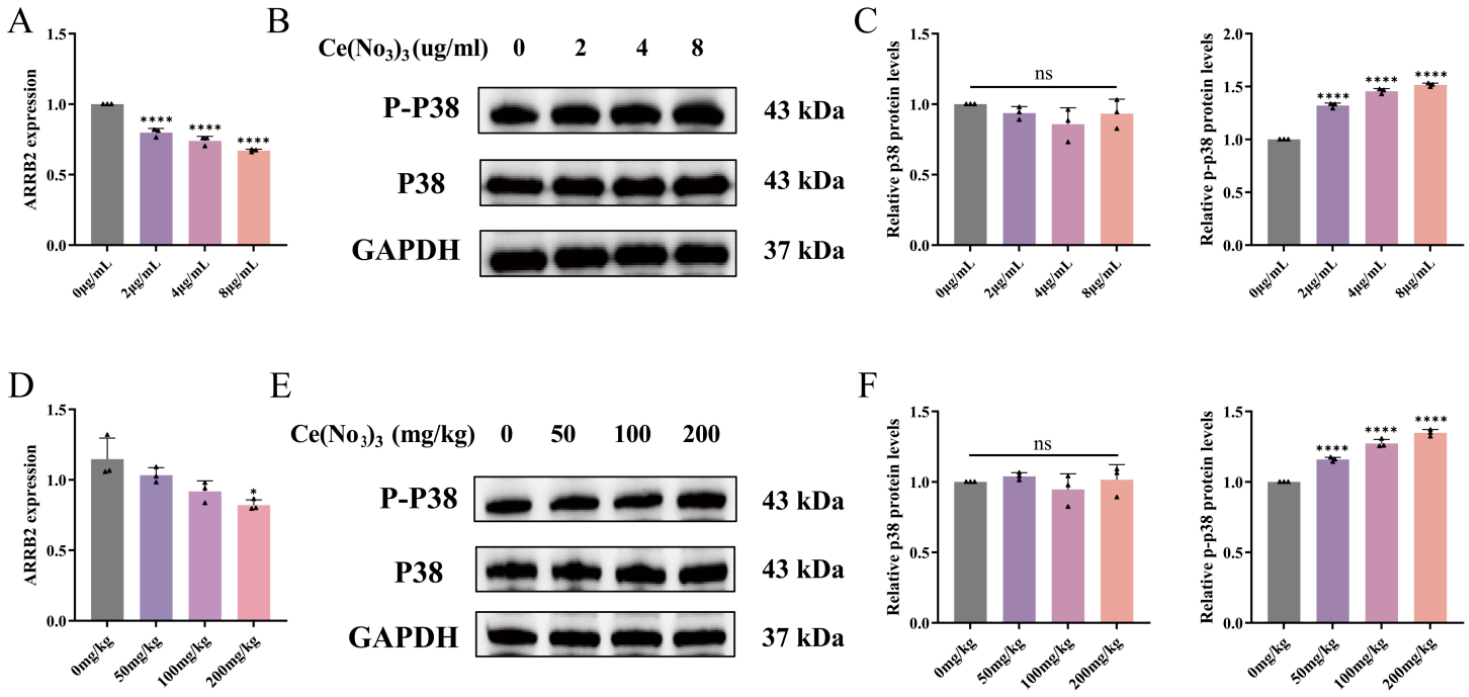


Figure 7

Cerium exposure activates the MAPK signaling pathway.Figure X. $Ce(NO_3)_3$ activates the P38 MAPK pathway in vitro and in vivo.(A) Relative expression of ARRB2 in JEG-3 cells treated with 0, 2, 4, or 8 μg/mL $Ce(NO_3)_3$ for 24 h, measured by qPCR.(B) Representative Western blot images showing phosphorylated P38 (P-P38), total P38, and GAPDH in JEG-3 cells treated with increasing concentrations of $Ce(NO_3)_3$.(C) Quantification of P-P38/P38 ratio and relative P-P38 protein levels in $Ce(NO_3)_3$-treated JEG-3 cells.(D) Relative expression of ARRB2 in placental tissues from rats treated with $Ce(NO_3)_3$ (0, 50, 100, or 200 mg/kg), measured by qPCR.(E) Western blot analysis of P-P38, total P38, and GAPDH in rat placentas after $Ce(NO_3)_3$ exposure.(F) Quantification of P-P38/P38 ratio and relative P-P38 protein levels in placental tissues.Data are presented as mean ± SD of three independent experiments. *p < 0.05, **p < 0.01, ****p < 0.0001

Supplementary Files

This is a list of supplementary files associated with this preprint. Click to download.

- OriginalWesternBlotimage.pdf